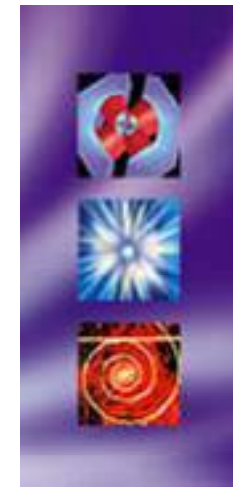


Vacuum-Related Electron Cloud Issues

Oleg B. Malyshev

ASTeC

Daresbury Laboratory



Outline

1. **Dynamic vacuum due to SR**
2. **Vacuum-Related Electron Cloud Issues**
3. **Ion induced pressure instability in positron DR**

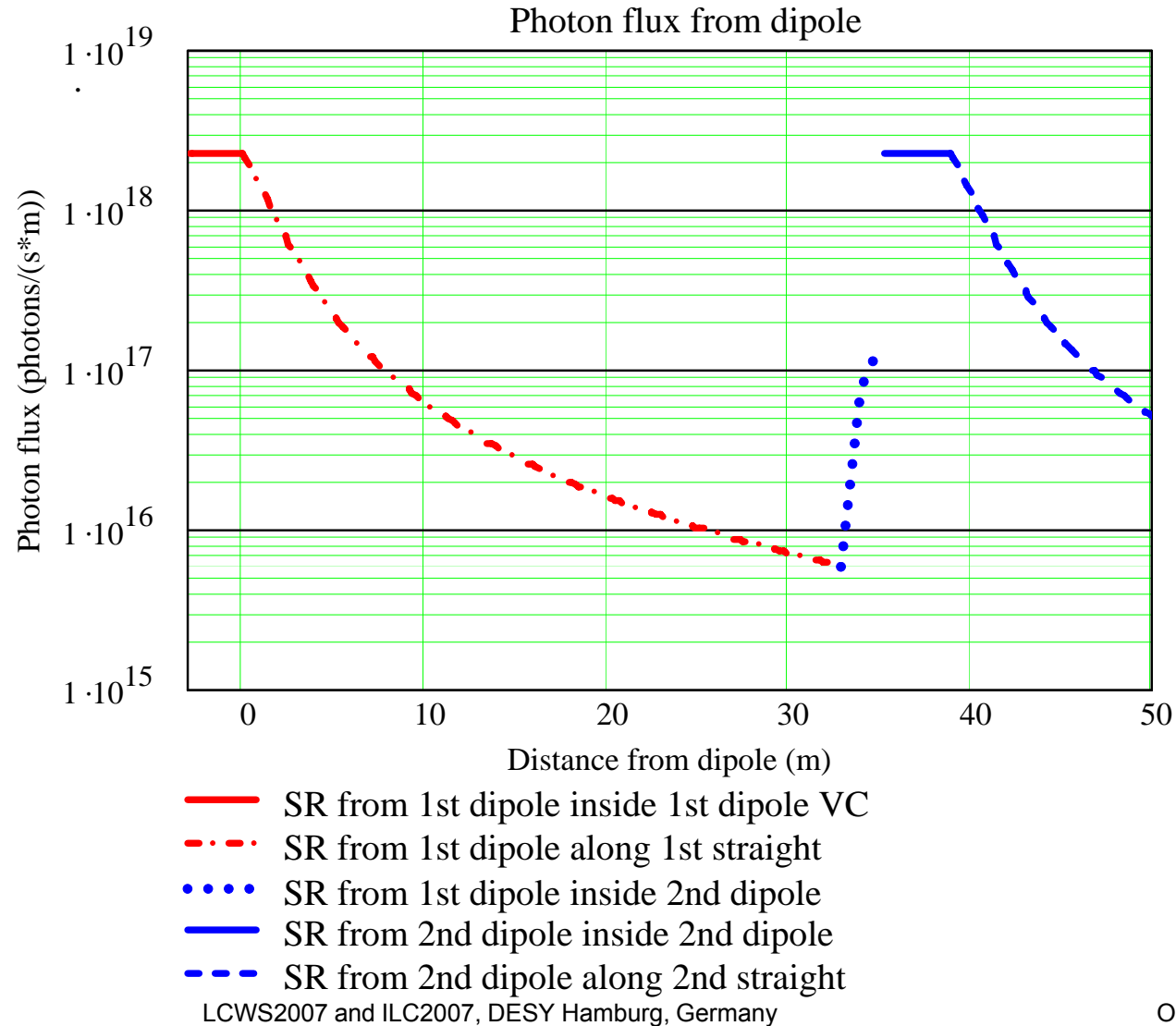
Vacuum required for ILC DRs

- The need to avoid fast ion instability leads to very demanding specifications for the vacuum in the electron damping ring [Lanfa Wang, private communication]:
 - < 0.5 nTorr CO in the arc cell,
 - < 2 nTorr CO in the wiggler cell and
 - < 0.1 nTorr CO in the straight section
- In the positron damping ring required vacuum level was not specified and assumed as 1 nTorr (common figure for storage rings)

SR photon induced dynamic pressure

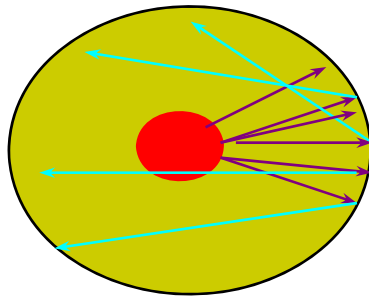
- SR induced gas desorption is the main source of gas defining dynamic pressure SR sources and colliders

Photon flux onto the 50-mm diameter vacuum chamber walls inside the ILC DR dipoles and along the short straights



Tubular chamber vs. a vacuum chamber with an antechamber

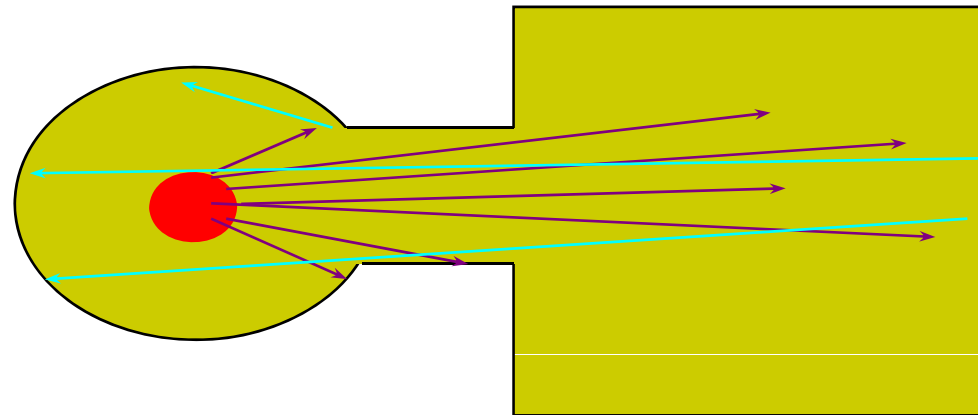
Tubular chamber



Diffuse reflected photons irradiate all surface (from **1.5% to 20%**)

Forward scattered photons from 2% to 65%

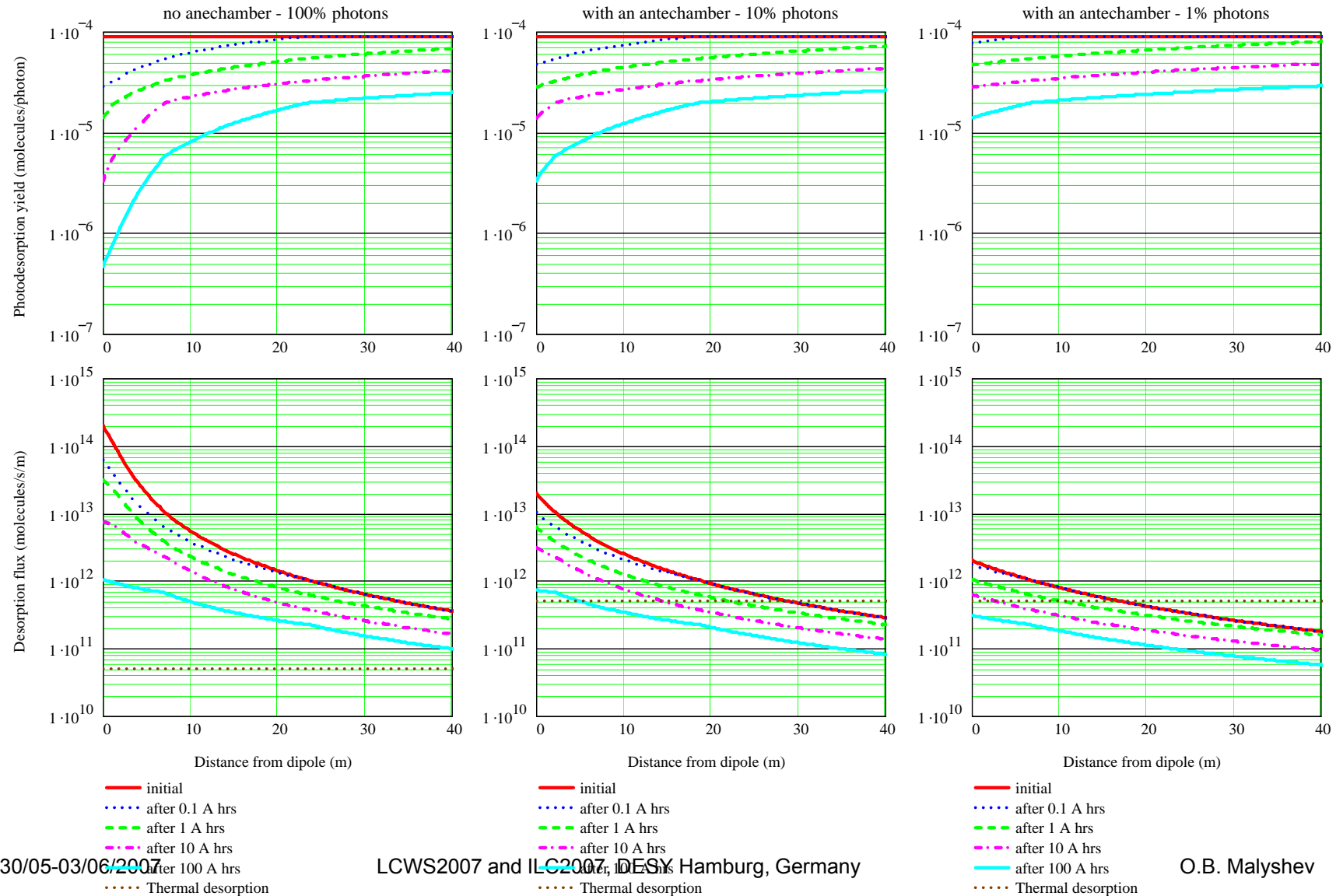
Vacuum chamber with an antechamber



~1-10% of photons hit a beam vacuum chamber

- **~99-90%** of photons enter an ante-chamber,
- thermal induced desorption is much larger (proportional to the surface area).

Outgassing from baked *in-situ* tubular chamber vs a vacuum chamber with antechamber (outgassing from an SR absorber is not included)

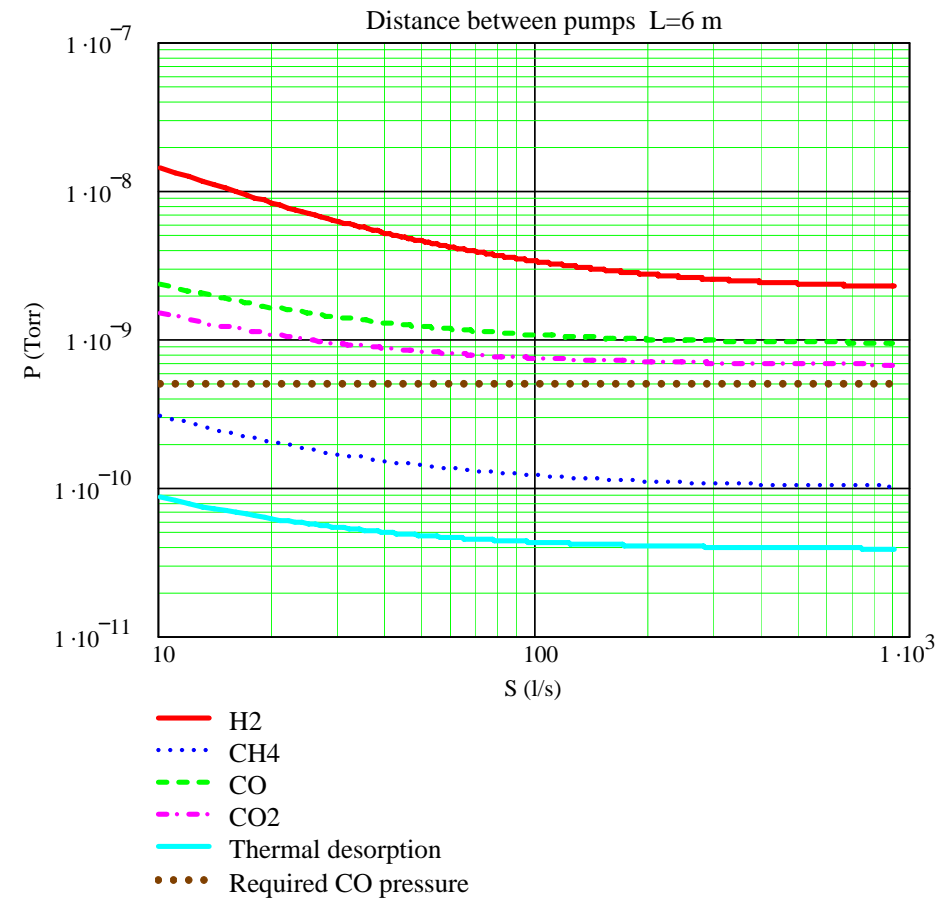
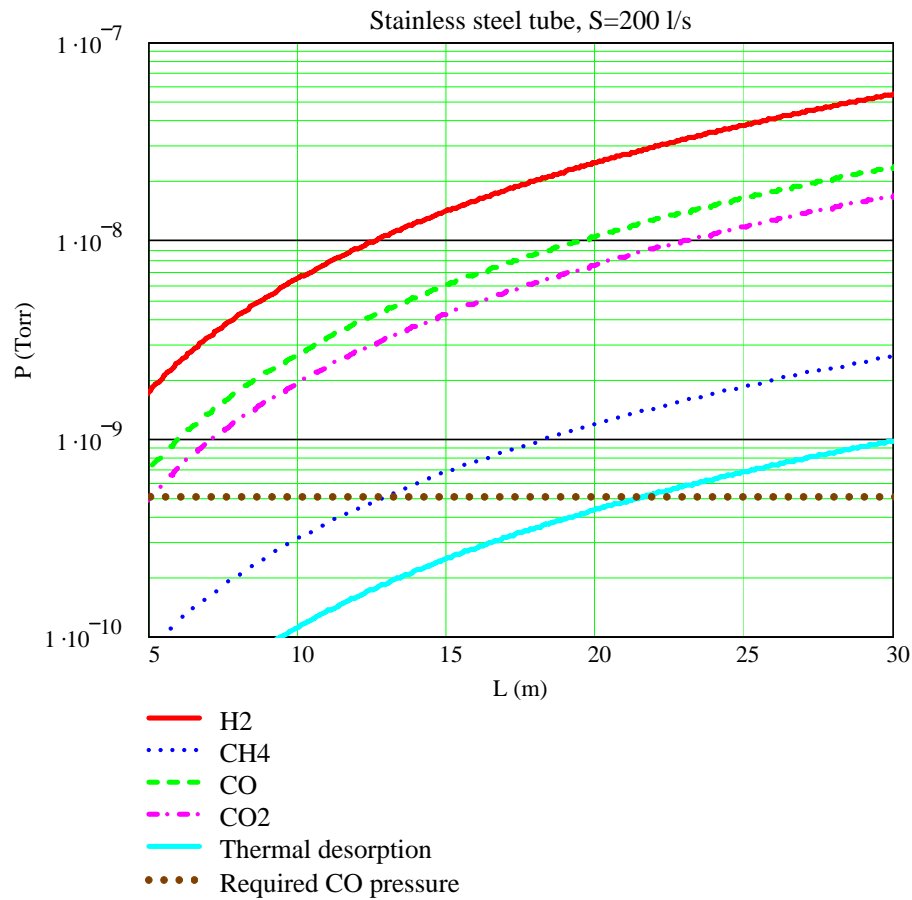


Vacuum: tubular chamber vs a vacuum chamber with an antechamber

- Results:
 - The distributed gas desorption after 100 Ahr of beam conditioning is almost the same with and without antechamber.
 - Thermal outgassing is a few times larger with an ante-chamber
 - Photon stimulated desorption from the lumped absorber in the ante-chamber.
 - => The total outgassing inside the vacuum chamber with an ante-chamber is larger.
- An ante-chamber design:
 - Does indeed increase the vacuum conductance (+)
 - Allows installing lumped SR power absorbers (+)
 - Does not help in reducing the SR induced out-gassing after 100 Ahr conditioning (–)
 - Larger thermal desorption (–)
 - Requires larger pumps (–)
 - More expensive (–)

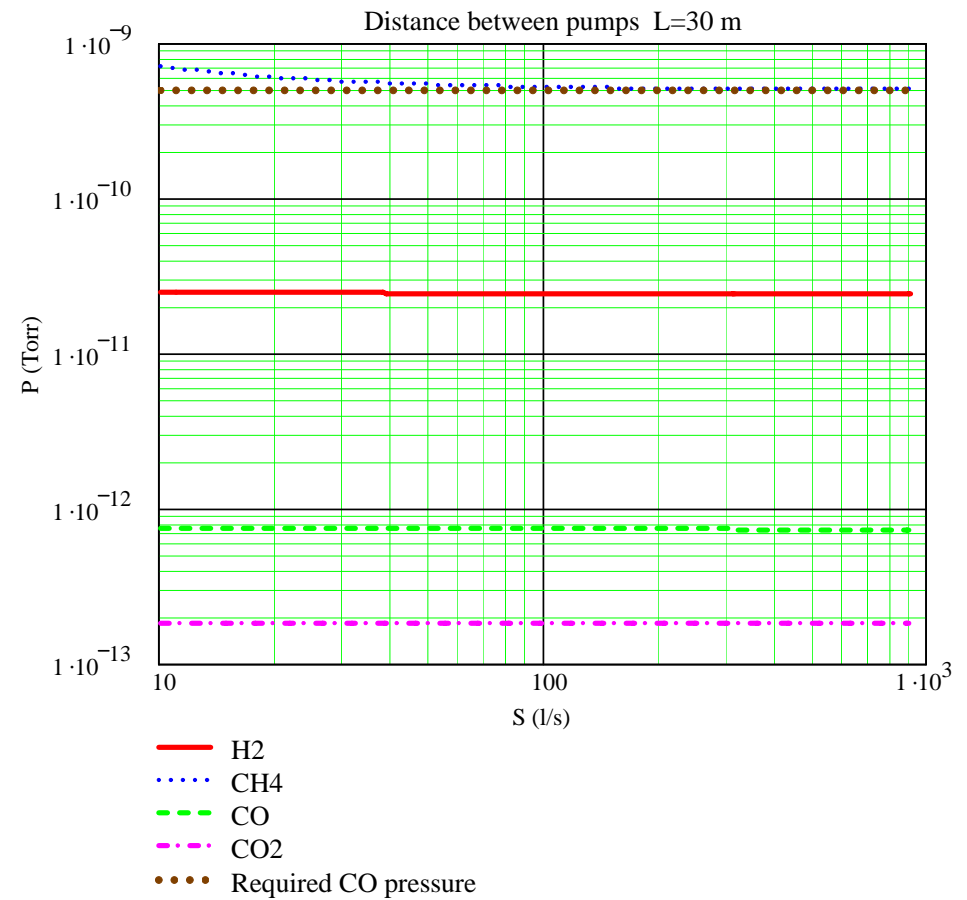
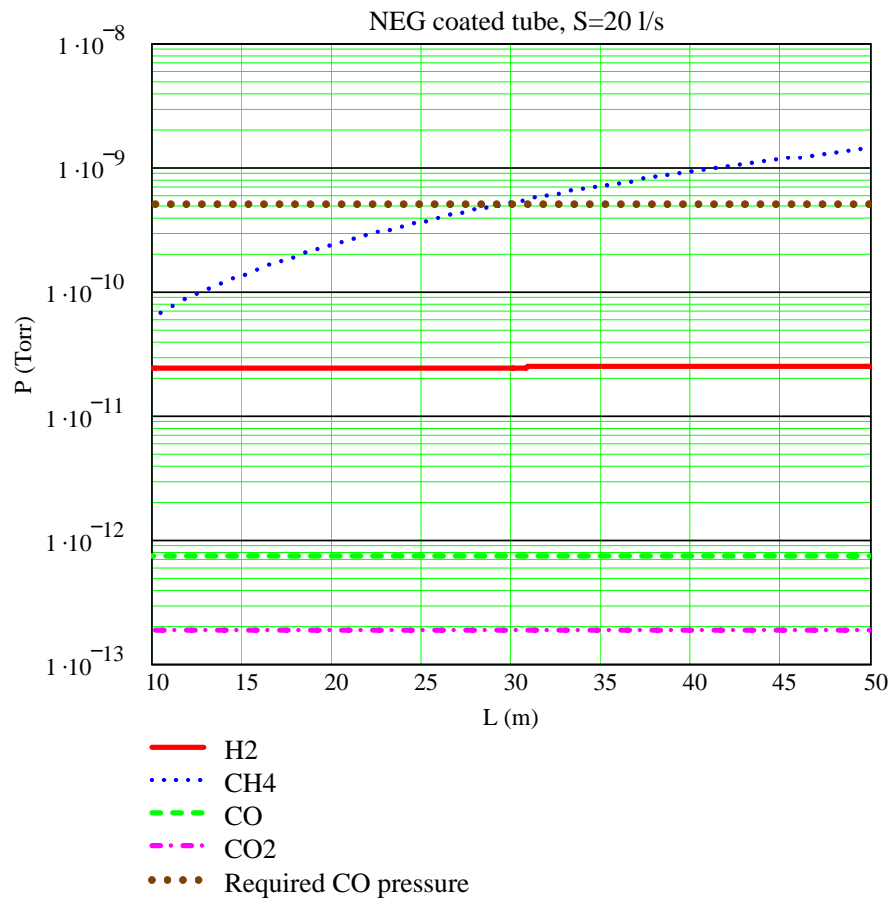
Pressure along the arc: inside a stainless steel tube

after 100 Ahr beam conditioning: $S_{\text{eff}} = 200 \text{ l/s}$ every 5 m



Pressure along the arc: inside a NEG coated tube

after 100 Ahr beam conditioning: $S_{\text{eff}} = 20 \text{ l/s}$ every 30 m



Main results of the modelling with SR only

- NEG coating of vacuum chamber along both the arcs and the wigglers as well as a few tens meters downstream of both looks to be the only possible solution to fulfil vacuum requirement for the ILC dumping ring

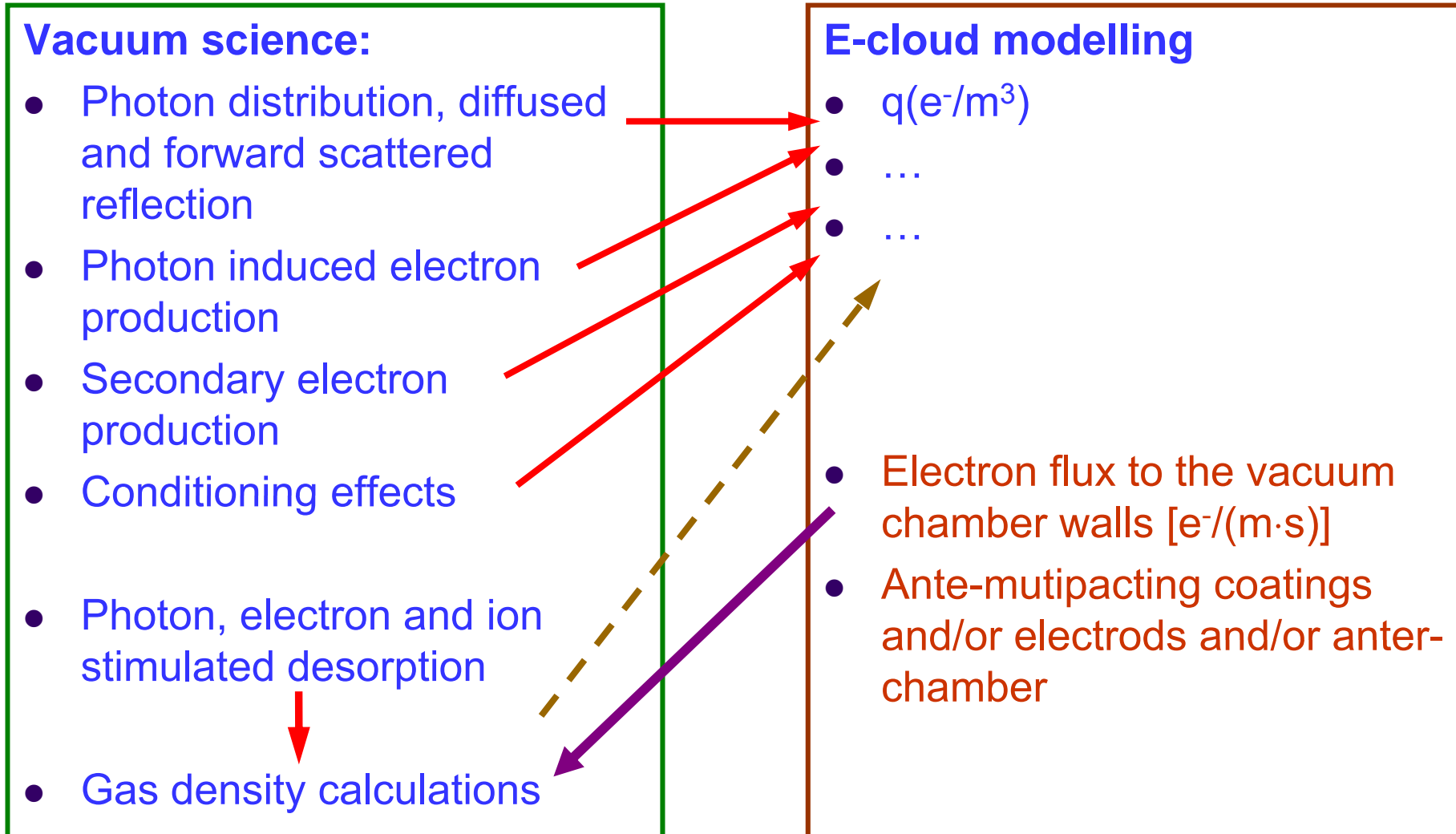
Ideal vacuum chamber for vacuum design:

- Round or elliptical tube
 - Cheapest from technological point of view
- No antechamber if SR power can be absorbed with vacuum chamber wall cooling
 - Beam conditioning is most efficient
 - Easy geometry for TiZrV coating
- NEG coated
 - Requires less number of pumps with less pumping speed
 - 180°C for NEG activation instead of 250-300°C bakeout
 - Choice of vacuum chamber material (stainless steel, copper and aluminium) does not affect vacuum in this case
 - Residual gas CH₄ and H₂ (almost no CO and CO₂)

Ante-chamber

- An ante-chamber design is not required for vacuum to deal with photon induced desorption
- Ante-chamber is required in wigglers to deal with high SR power
- An ante-chamber might be beneficial for e-cloud suppression in the wigglers and dipoles (to reduce PEY parameter in the model)
- A vacuum chamber with an ante-chamber
 - is more expensive than a round or elliptical tube
 - beam conditioning is much less efficient
 - difficult (but possible) geometry for TiZrV coating

Vacuum studies vs e-cloud modelling



Photon reflectivity and azimuthal distribution

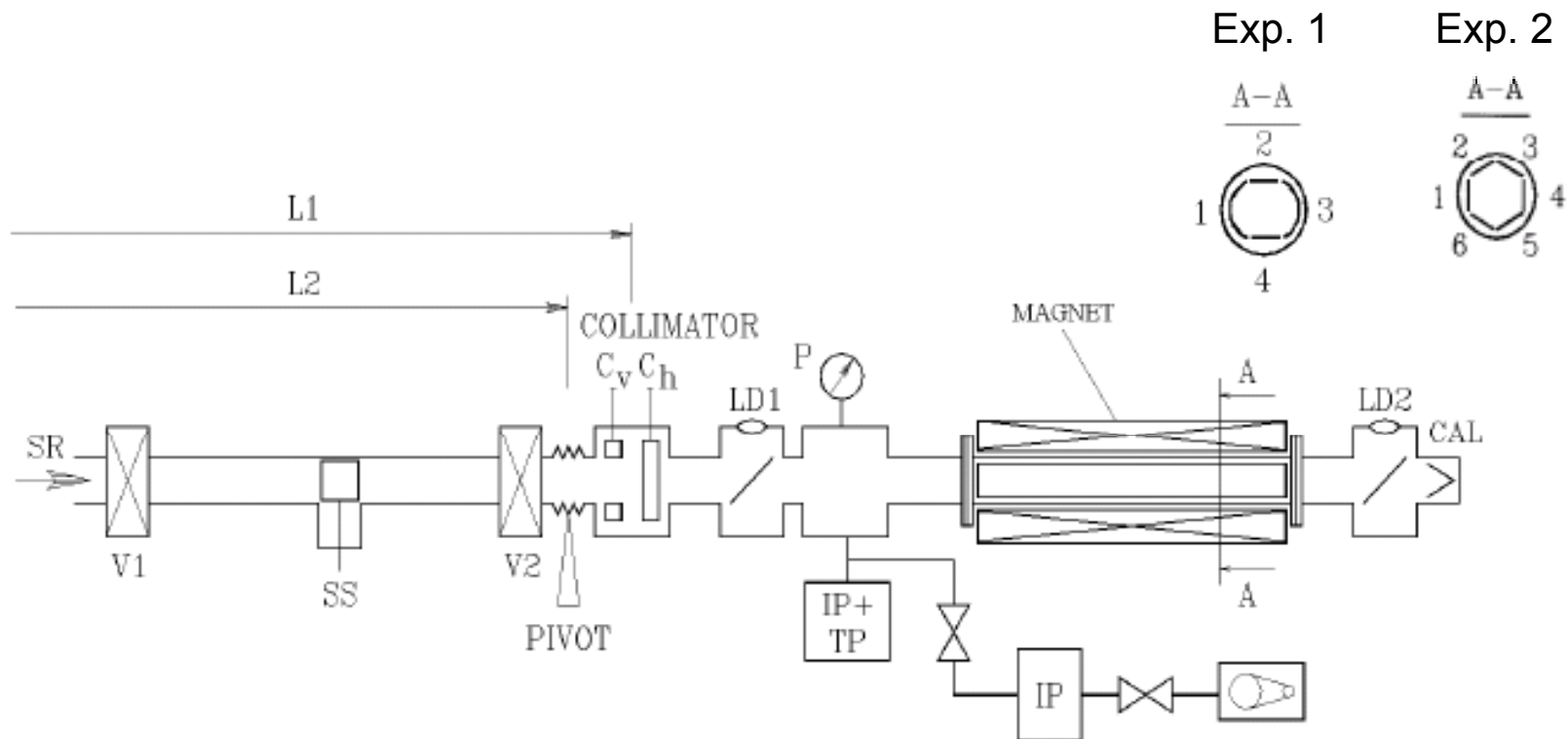


Figure 1. Set-up for measurements of the azimuthal photoelectron distribution in magnetic field and of the photon reflectivity

Forward scattered reflectivity at 20 mrad grazing incidence

	Sample Reflectivity (power) (%)	Reflectivity (photons) (%)
Stainless steel as-received	2	22
Cu co-laminated as-received	50	95
Cu co-laminated oxidised	20	65

I.e. the reflected photons are mainly low energy photons

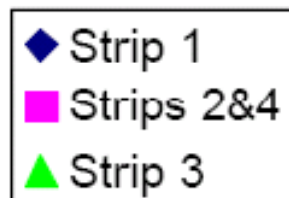
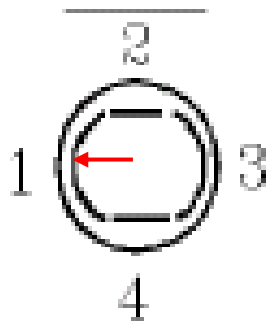
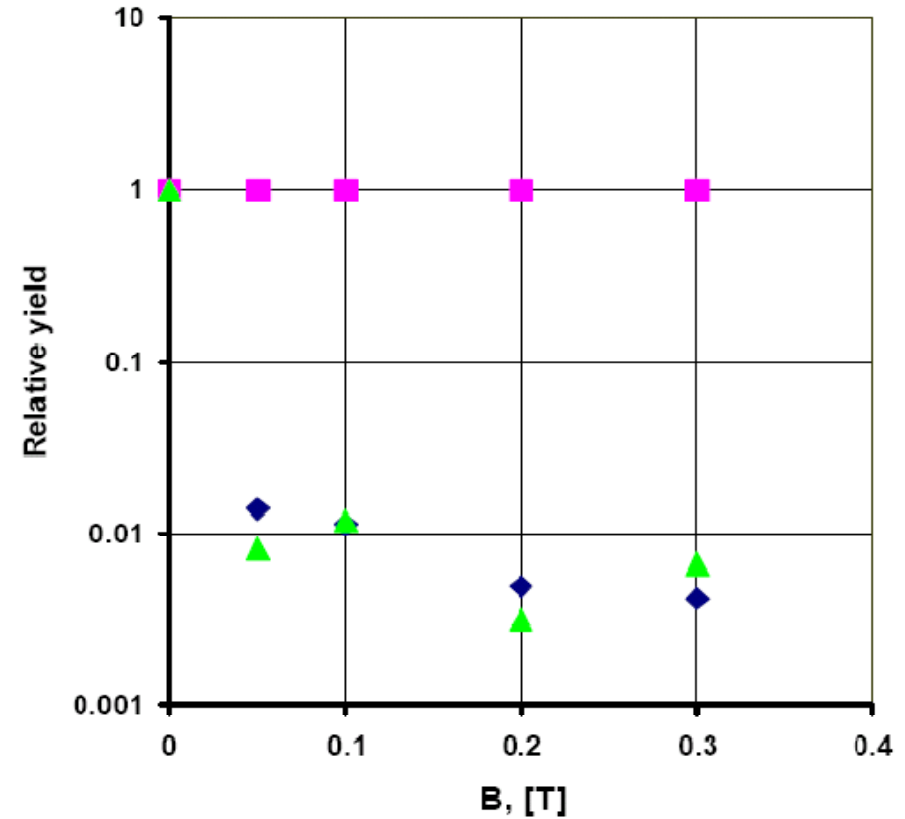
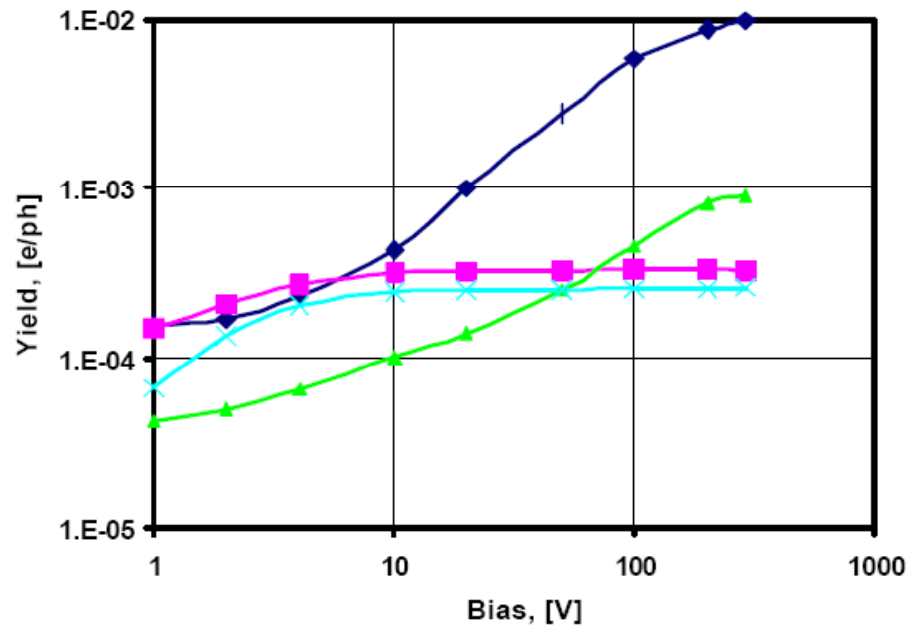
V.V. Anashin et al. / Nuclear Instruments and Methods in Physics Research A 448 (2000) 76-80.

See also: V. Baglin, I.R. Collins, O. Grobner, EPAC'98, Stockholm, June 1998.

Photon azimuthal distribution – 6 strips experiment

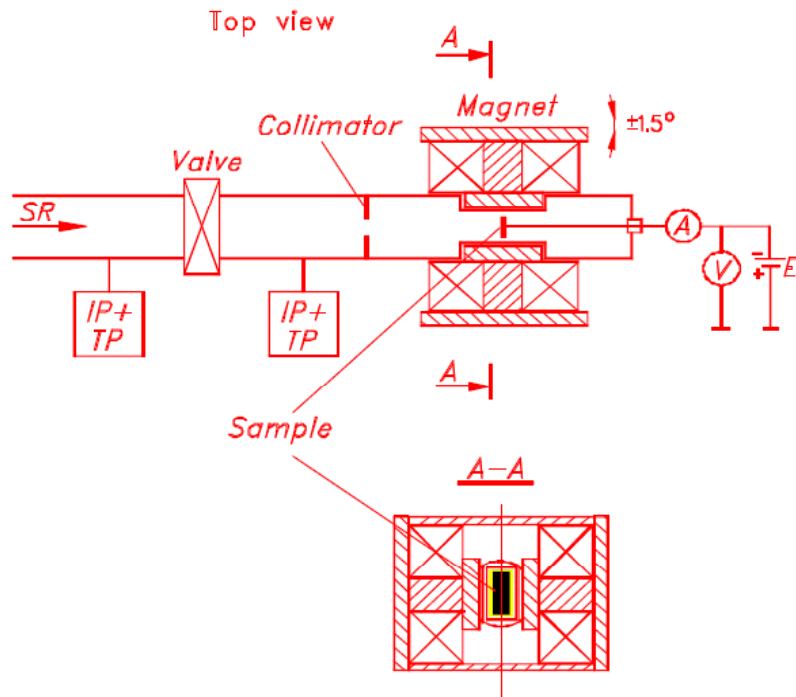
Sample	ϵ_c (eV)	Strip 1	Strip 2 or Strip 3	Strip 4 or Strip 5	Strip 6
$I_i / \sum_{i=1}^6 I_i$					
Stainless steel	243	74	3.8	8	2.5
Bright Cu	245	90	1.9	2	1.8
Oxidised Cu	205	95	1	1.1	1
$I_i(1-R) / \sum_{i=1}^6 I_i$					
Stainless steel	243	60	2.5	6.0	1.5
Bright Cu	245	4.5	0.1	0.1	0.1
Oxidised Cu	205	30	0.3	0.4	0.3

Photon azimuthal distribution – 4 strips experiment



V.V. Anashin, O.B. Malyshev, N.V. Fedorov and A.A. Krasnov.
 Azimuthal distribution of photoelectrons for an LHC beam screen prototype in a magnetic field. Vacuum Technical Note 99-06. LHC-VAC, CERN April 1999.

Photoelectron current in magnetic field



V.V. Anashin, O.B. Malyshev, N.V. Fedorov and A.A. Krasnov. Photoelectron current in magnetic field. Vacuum Technical Note 99-03. LHC-VAC, CERN April 1999.

- Sample SS. The stainless steel sample made from a rolled sheet.
- Sample Cu/SS-1 (=). The copper laminated stainless steel made from a sheet; the rolling lines are across the sample.
- Sample Cu/SS-2 (|||). The copper laminated stainless steel made from a sheet; the rolling lines are along the sample.
- Sample Cu/SS-3 (||| ox). The copper laminated stainless steel made from a sheet; the rolling lines are along the sample. Oxidation.
- Sample Cu/SS-4 (___ /). The copper laminated stainless steel made from a sheet with turned-in, long edges, i.e. 5-mm wide strips at the long edges were turned to 10–15° towards the SR; the rolling lines are along the sample.
- Sample OFHC (⊥⊥⊥). The copper sample machined from a bulk OFHC with ribs along the sample. No special treatment. The ribs are 1 mm in height and
- 0.2 mm in width. The distance between the ribs is 3 mm.
- Sample Au/SS. The stainless steel sample electro-deposited with 6- μ m Au.

Results

1) The photoelectron yield is different for studied samples at zero potential, but the same at the accelerating potential of 300V,

$k = (1.5 \pm 0.3) \times 10^{-2} \text{ e}^-/\gamma$. The photoelectron yield from the layer of gold is about two times higher.

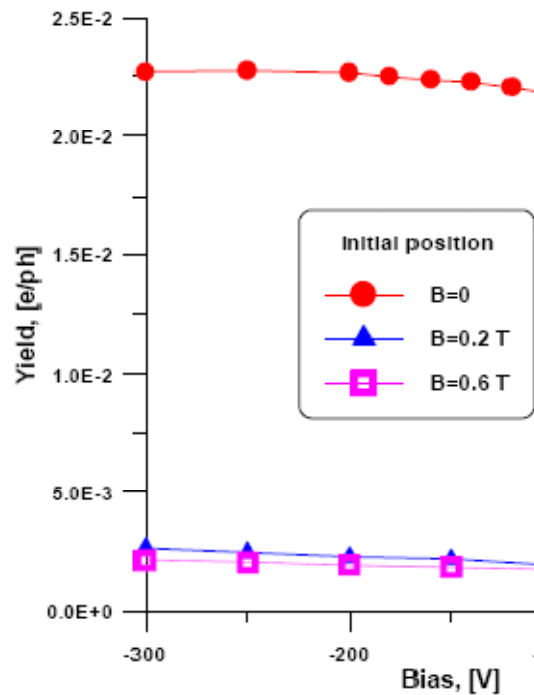
2) The magnetic field suppresses the photoelectron yield up to **30–100 times** when the surface is parallel to the magnetic field, but this effect is much less at the angle of 1.5° (5–10 times).

3) The photoelectron yield decreases with the accumulated photon dose: the photoelectron yield reduced 2–3 times at the accumulated photon dose of about $10^{22} \text{ photons/cm}^2$.

Experiment No. and Sample	Beams		Measurements without magnetic field			Magnetic field efficiency:	
	E_{e^+} , [MeV]	E_c , [eV]	κ ; [e ⁻ /γ] U=-300V	$\frac{\kappa(0V)}{\kappa(-300V)}$	Reflectivity $\frac{\kappa(+300V)}{\kappa(-300V)}$	U = 0 $\frac{\kappa(0.6T)}{\kappa(0T)}$	U = -300V $\frac{\kappa(0.6T)}{\kappa(0T)}$
Exp. 1, SS	518	259	0.016	0.036	0.024	0.023	0.028
Exp. 2, Cu/SS-1 (≡)	514	253	0.015	0.15	0.044	0.010	0.029
Exp. 3, Cu/SS-2 ()	470	194	0.014	0.11	0.015	0.021	0.030
Exp. 4, Cu/SS-3 (ox)	392	112	0.014	0.052	0.033	0.018	0.015
Exp. 5, OFHC (⊥⊥⊥)	380	102	0.0084	0.055	0.023	0.024	0.013
Exp. 6, Cu/SS-4 (∧_/_)	220	20	0.014	0.07	—	0.02	0.06
Exp. 7, Cu/SS-4 (∧_/_)	560	319	0.018	0.05	0.180	0.01	0.08
Exp. 8, Au/SS	580	356	0.027	0.06	0.045	0.028	0.042

Examples of measurement results

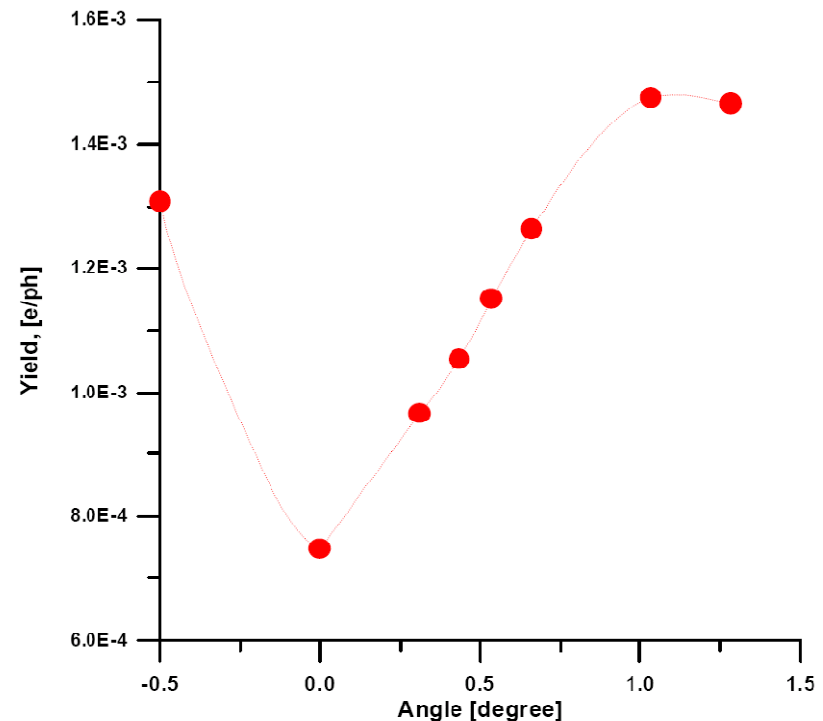
Exp. 1.1. Photoelectron emission from stainless steel sample in magnetic field



PEY (and SEY) depends on potential gradient at the surface!

30/05-03/06/2007

Exp.2. Copper laminated stainless steel. Dependence on angle between substrate surface and magnetic field.



Grooves alignment in respect to magnetic field

O.B. Malyshev

Input parameters in e-cloud models

- Photon distribution, diffused and forward scattered reflection
- Photon induced electron production
 - *there are no data directly related to the ILC DR (i.e. measured at 3 and 30 keV),*
 - *there are no data for NEG coated and TiN coated surfaces,*
 - *the access to SR beamline and volunteers to perform a study are required*

Input parameters in e-cloud models

- Photon distribution, diffused and forward scattered reflection
- Photon induced electron production
- Secondary electron production
 - The uncertainties here are almost the same as with photons:
 - Secondary electron yields depend on the potential gradient near the surface (Most likely, similar to PEY, SEY increases up to 10-20 times in the presence of accelerating potential)
 - Secondary electron yields depend on the magnetic field near the surface (Most likely, similar to PEY, SEY decreases up to 2-20 times in the presence of the magnetic field parallel to the surface)
 - Choice of material: NEG coated surfaces was not well studied yet, it is still not clear what is better (i.e. lower SEY) NEG TiZrV coating or TiN coating.

Input parameters in e-cloud models

- Photon distribution, diffused and forward scattered reflection
- Photon induced electron production
- Secondary electron production
- Conditioning effects
- Effect of beam electric field
- Effect of magnetic field

All these parameters

- are not well experimentally evaluated for the ILC-DR conditions
- vary in wide range depending on material, geometry, history, etc.

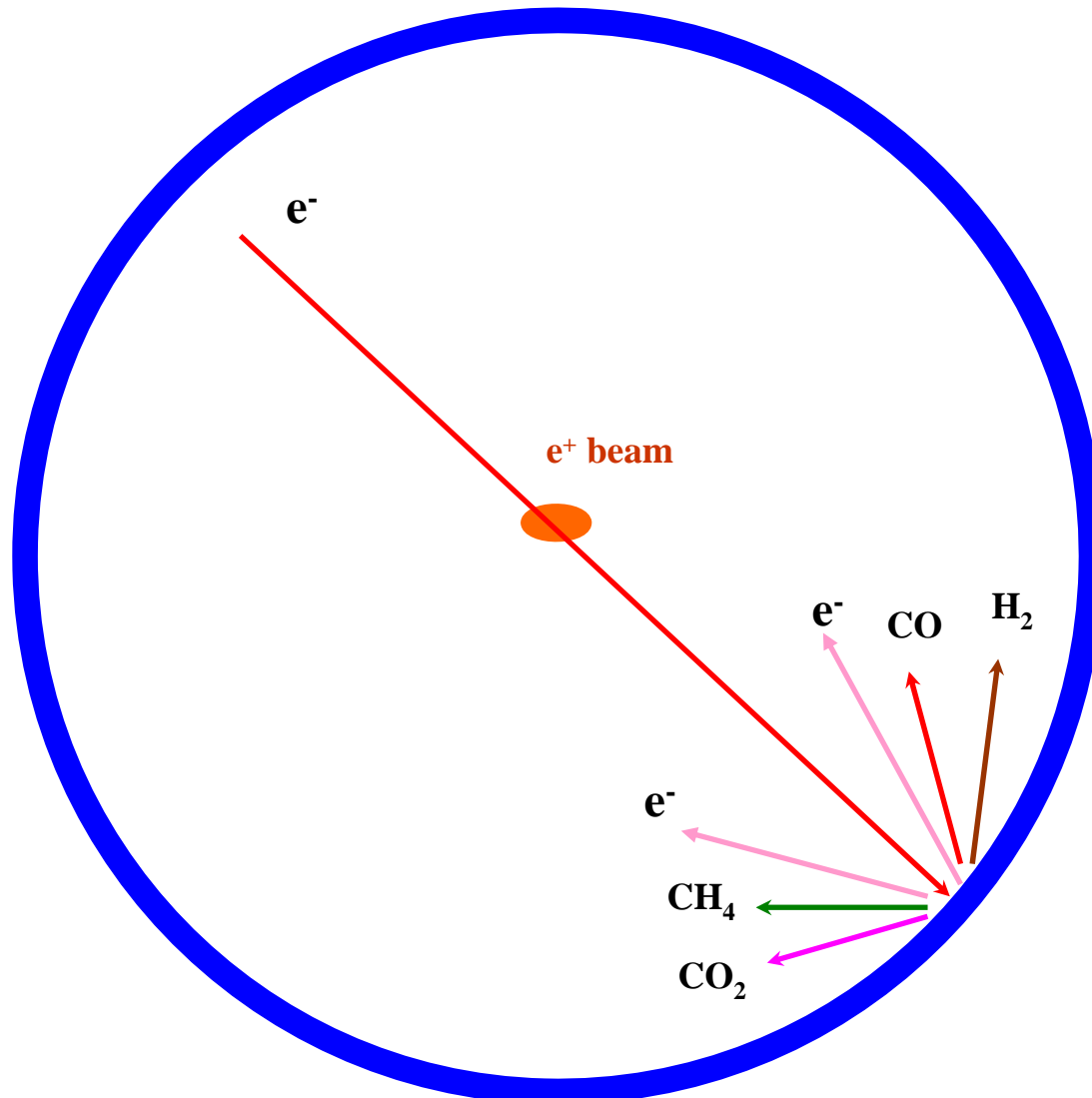
Input parameters in e-cloud models

- Photon distribution, diffused and forward scattered reflection
- Photon induced electron production
- Secondary electron production
- Conditioning effects
- Effect of beam electric field
- Effect of magnetic field

All these parameters

- are not well experimentally evaluated for the ILC-DR conditions
- vary in wide range depending on material, geometry, history, etc.
- Experiments with SR are planned to perform on VEPP-3 at $\varepsilon_c = 4.5$ keV at BINP (Novosibirsk, Russia)

How the e-cloud affect vacuum



How the e-cloud affect vacuum

- The electron flux $\Phi \sim 10^{16}$ e⁻/(s·m) with $E \approx 200$ eV (0.3 W) will desorb approximately the same gas flux as the photon flux of $\sim 10^{18}$ γ /(s·m) from a DR dipole.
- If the electron simulated desorption is larger than photon stimulated desorption, that should be considered in vacuum design and conditioning scenario.
- Gas density will increase => gas ionisation will also increase =>
 - Electrons are added to e-cloud
 - Ions are accelerated and hit the wall of vacuum chamber => ion induced gas desorption and secondary electron production
- Gas density increase may change e-cloud density.

How the e-cloud affect vacuum

- Grooves and antechamber will increase the necessary conditioning time and complicate the TiZrV coating. It is more expensive than NEG coated tube.
- Electrodes and insulating materials may dramatically increase the gas density in a vacuum chamber due to thermal, photon, electron and ion induced gas desorption.
 - Choice of material and design must be UHV compatible.
 - The NEG coating might be difficult, impossible or inefficient, which will lead to much more expensive vacuum design.
 - If the 'e-cloud killer' requires a vertical space – it will require larger magnet gap and more expensive dipoles.

If e-cloud is too large in a round tube

- Defining what is the main source of electrons:
 - Photo-electrons
 - Geometrical: reduction or localisation of direct and reflected photons
 - Surface treatment, conditioning, coating
 - Secondary electrons
 - All possible solution discussed during this workshop
 - Gas ionisation
 - Surface treatment and conditioning
 - Low outgassing coating
 - Better pumping
- A complex solution for vacuum and e-cloud problem:
 - Good solution against Photo-electrons or Secondary electrons might lead to higher gas density and higher gas ionisation, and vice versa.

W. Bruns's results for the arc

SEY	q [e ⁻ /m ³]				Power [W/m]			
	PEY [e ⁻ / (e ⁺ ·m)]				PEY [e ⁻ / (e ⁺ ·m)]			
	10 ⁻⁴	10 ⁻³	0.01	0.1	10 ⁻⁴	10 ⁻³	0.01	0.1
1.1	2·10 ¹¹	2·10 ¹²	1·10 ¹³	5·10 ¹³	0.3	3	30	80
1.3	3·10 ¹²	2·10 ¹³	3·10 ¹³	5·10 ¹³	2	30	80	100
1.5	3·10 ¹²	5·10 ¹³	5·10 ¹³	5·10 ¹³	80	80	100	100
1.7	5·10 ¹²	5·10 ¹³	5·10 ¹³	5·10 ¹³	80	100	100	100

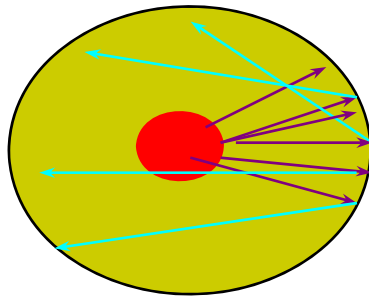
Increase of both PEY and SEY lead to multipacting,
pressure increase might also be important

PEY – the tube without a magnetic field

- Generated photons hitting vacuum chamber walls:
 - $\Gamma = 0.9 \gamma/e^+$ in the arc and shortly downstream straight
 - $\Gamma = 10 \gamma/e^+$ in the wiggler and shortly downstream straight
- Photo-electron emission coefficient:
 - $\kappa = 0.01-0.1 e^-/\gamma$ depending on material, magnetic and electric field and photon energy
 - κ is unknown for NEG coating
- PEY
 - $PEY_{ds} = 0.01-0.1 e^-/e^+$ in a tubular chamber in the arc straight downstream a dipole
 - Required ???
 - $PEY_{ws} = 0.1-1 e^-/e^+$ in a tubular chamber in the straight downstream a wiggler
 - Required ???

PEY: tubular chamber vs. a vacuum chamber with an antechamber

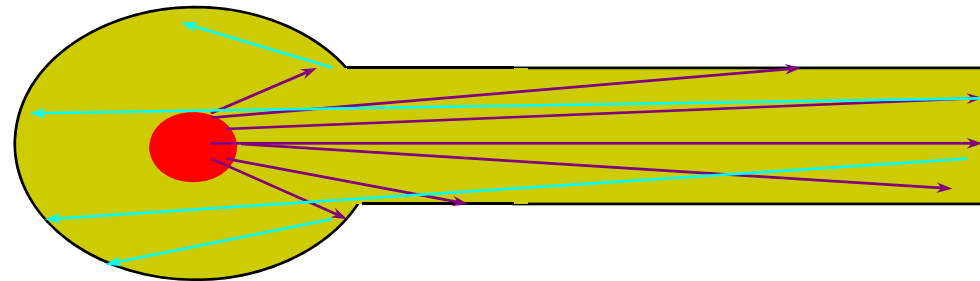
Tubular chamber



Diffuse reflected photons irradiate all surface (from 1.5% to 20%)

Forward scattered photons from 2% to 65%

Vacuum chamber with an antechamber



~1-10% of photons hit a beam vacuum chamber,

Some of photons entered an ante-chamber might be diffused or back/forward scattered to the beam chamber

PEY – tube with a magnetic field

- Generated photons hit vacuum chamber walls:
 - $\Gamma = 0.9 \gamma/e^+$ in the arc and shortly downstream straight
 - $\Gamma = 10 \gamma/e^+$ in the wiggler and shortly downstream straight
- Photons reflected/scattered after first hit with walls:
 - $R = 3\%–65\%$ (material, treatment, geometry)
- Photo-electron emission coefficient:
 - $\kappa = 0.01–0.1 e^-/\gamma$ depending on material, magnetic and electric field and photon energy
 - κ is unknown for NEG coating
- PEY
 - $PEY_d = 3 \cdot 10^{-4} – 0.065 e^-/e^+$ in a tubular chamber in a dipole (+/-)
 - Required $\sim 10^{-4} e^-/e^+$
 - $PEY_{ws} = 3 \cdot 10^{-3} – 0.65 e^-/e^+$ in a tubular chamber in the straight downstream a wiggler (-)
 - Required $\sim 10^{-4} e^-/e^+$

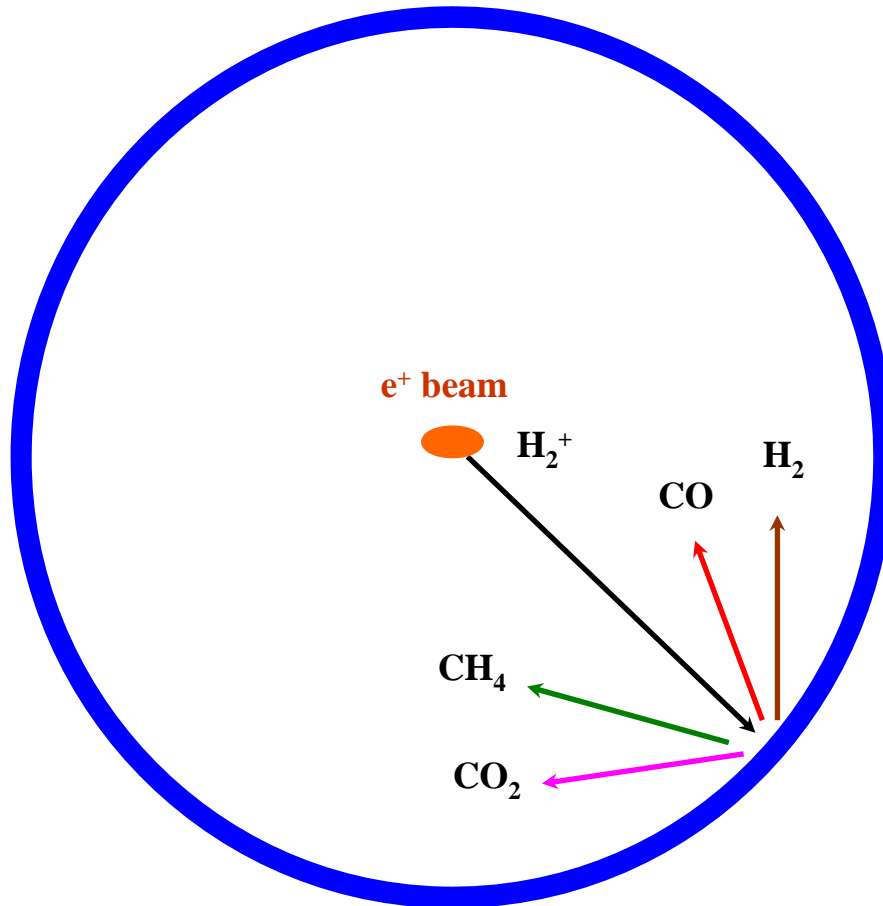
PEY – vac. chamber with a KEKB-type ante-chamber in a magnetic field

- Generated photons hit vacuum chamber walls:
 - $\Gamma = 0.9 \gamma/e^+$ in the arc and shortly downstream straight
 - $\Gamma = 10 \gamma/e^+$ in the wiggler and shortly downstream straight
- Photons absorbed in the beam chamber:
 - $F = 1\%–10\%$ (material, treatment, geometry)
- Photons reflected/scattered after first hit with beam chamber walls:
 - $R = 3\%–65\%$ (material, treatment, geometry)
- Photo-electron emission coefficient:
 - $\kappa = 0.01–0.1 e^-/\gamma$ depending on material, magnetic and electric field and photon energy
 - κ is unknown for NEG coating
- PEY
 - $PEY_d = 3 \cdot 10^{-6} – 6.5 \cdot 10^{-3} e^-/e^+$ in a vacuum chamber in a dipole (+)
 - Required $\sim 10^{-4} e^-/e^+$
 - $PEY_{ws} = 3 \cdot 10^{-5} – 6.5 \cdot 10^{-2} e^-/e^+$ in a vacuum chamber in a wiggler (+)
 - Required $\sim 10^{-4} e^-/e^+$

Ante-chamber vs. PEY

- To reach required value for a parameter PEY a KEKB-type antechamber
 - Is required in wigglers
 - Can help in the arc dipoles

Ion induced pressure instability in the positron ring



$$P = \frac{Q}{S_{eff} - \chi \frac{\sigma I}{e}}$$

where

Q = gas desorption,

S_{eff} = effective pumping speed,

χ = ion induced desorption yield

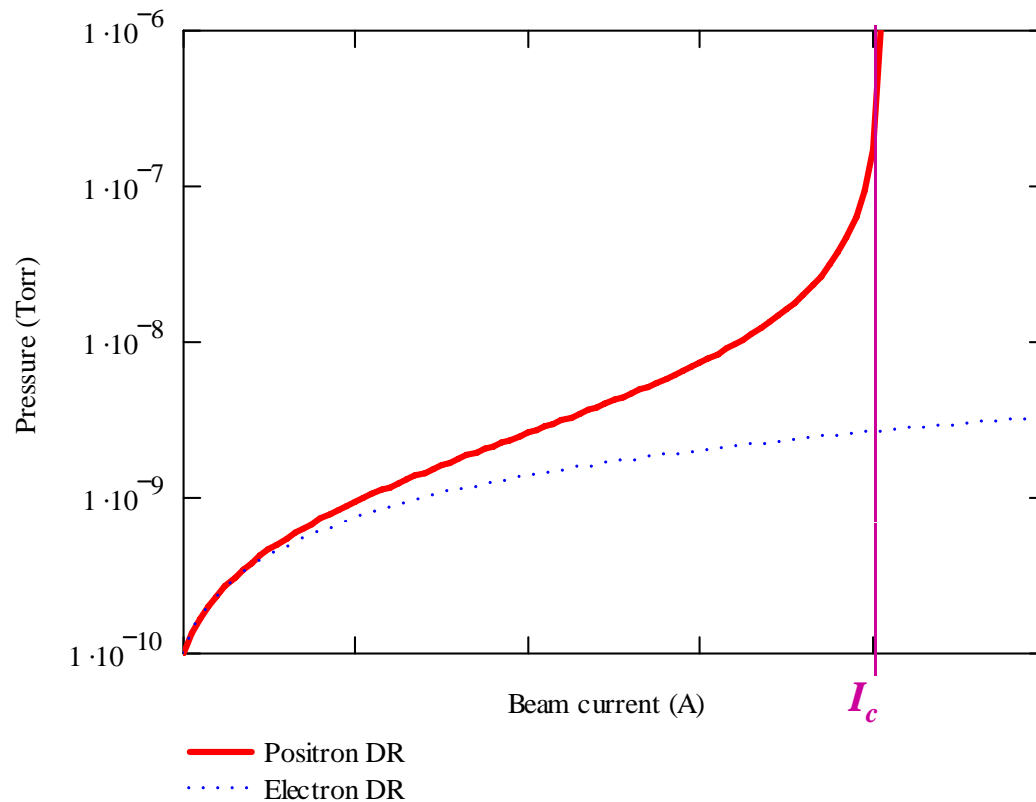
σ = ionisation cross section,

I = beam current.

$$\chi = f(E_{ion}, M_{ion}, material, bakeout, \dots)$$

$$E_{ion} = f(N_{bunch}, \tau, T, \sigma_x, \sigma_y, \dots)$$

Critical current



Critical current, I_c , is a current when pressure (or gas density) increases dramatically.

Mathematically, if

$$P = \frac{Q}{S_{eff} - \chi \frac{\sigma I}{e}}$$

when $S_{eff} > \chi \frac{\sigma I}{e}$

Hence $I < I_c$,

where $I_c = \frac{S_{eff} e}{\chi \sigma I}$

Ion energy at DR

The energy of ions reached at the end of damping cycle :

- Arcs: 220 – 270 eV
- Straights: 220 – 320 eV
- Wigglers: 320 – 340 eV

Corresponding ion induced desorption yields for Cu:

$$\chi = \begin{matrix} & \begin{matrix} \mathbf{H2,} & \mathbf{CH4,} & \mathbf{CO,} & \mathbf{CO2} \end{matrix} \\ \begin{pmatrix} 0.133 & 7.5 \times 10^{-3} & 0.047 & 0.015 \\ 0.433 & 0.028 & 0.233 & 0.075 \\ 0.717 & 0.05 & 0.467 & 0.15 \\ 0.867 & 0.065 & 0.65 & 0.21 \end{pmatrix} & \begin{matrix} \mathbf{H2+} \\ \mathbf{CH4+} \\ \mathbf{CO+} \\ \mathbf{CO2+} \end{matrix} \end{matrix}$$

Pressure instability thresholds:

- I_c – critical current
 - $I_c = \sim 0.8$ A for Cu tube, pump every 6 m
 - $I_c = \sim 2$ A for NEG coated tube, pump every 40 m
- L_c – critical length between pumps
 - $L_c = \sim 8$ m for Cu tube
 - $L_c = \sim 100$ m for NEG coated tube
- Hence,
 - For given parameters and large uncertainties, there is a possibility of ion induced pressure increase and even ion induced pressure instability in positron damping ring if pumping is insufficient.
 - There will be no ion induced pressure instability if TiZrV coating used

Conclusions

- An ante-chamber is not needed for vacuum (electron and positron DRs)
- A KEKB-type ante-chamber is required to suppress e-cloud in positron DR
 - in wigglers and, possibly, dipoles
 - the straight are to be studied
- Multipacting electrons in positron DR will cause the pressure increase comparable or larger than due to photons – to be considered in vacuum design
- Ion induced pressure instability might be a problem at ILC DR
 - Large distributed pumping speed required
 - TiZrV coated vacuum chamber has a sufficient safety margin